

EFEMP1 Expression Promotes *In vivo* Tumor Growth in Human Pancreatic Adenocarcinoma

Hendrik Seeliger,¹ Peter Camaj,¹ Ivan Ischenko,¹ Axel Kleespies,¹ Enrico N. De Toni,² Susanne E. Thieme,⁴ Helmut Blum,⁴ Gerald Assmann,³ Karl-Walter Jauch,¹ and Christiane J. Bruns¹

Departments of ¹Surgery and ²Gastroenterology and ³Institute of Pathology, Munich University Medical Center; ⁴Gene Center, Munich University, Munich, Germany

Abstract

The progression of pancreatic cancer is dependent on local tumor growth, angiogenesis, and metastasis. EFEMP1, a recently discovered member of the fibulin family, was characterized with regard to these key elements of pancreatic cancer progression. Differential gene expression was assessed by mRNA microarray hybridization in FG human pancreatic adenocarcinoma cells and L3.6pl cells, a highly metastatic variant of FG. *In vivo* orthotopic tumor growth of EFEMP1-transfected FG cells was examined in nude mice. To assess the angiogenic properties of EFEMP1, vascular endothelial growth factor (VEGF) production of tumor cells, endothelial cell proliferation and migration, and tumor microvessel density were analyzed in response to EFEMP1. Further, tumor cell apoptosis, cell cycle progression, and resistance to cytotoxic agents were quantitated by propidium iodide staining and flow cytometry. In microarray hybridization, EFEMP1 was shown to be significantly up-regulated in L3.6pl cells compared with FG cells. Concordantly, EFEMP1 transfection of FG cells stimulated orthotopic and metastatic tumor growth *in vivo*. EFEMP1 expression resulted in a stimulation of VEGF production by tumor cells and an increased number of CD31-positive microvessels. Endothelial cell proliferation and migration were not altered by EFEMP1, indicating an indirect angiogenic effect. Further, EFEMP1 expression decreased apoptosis and promoted cell cycle progression in response to serum starvation or exposure to gemcitabine, 5-fluorouracil, and irinotecan. EFEMP1 has protumorigenic effects on pancreatic cancer *in vivo* and *in vitro* mediated by

VEGF-driven angiogenesis and antiapoptotic mechanisms. Hence, EFEMP1 is a promising candidate for assessing prognosis and individualizing therapy in a clinical tumor setting. (Mol Cancer Res 2009;7(2):189–98)

Introduction

Pancreatic cancer is one of the leading causes of cancer-related deaths in western countries. Despite improved multimodal therapeutic regimens, its prognosis has improved only marginally, resulting in a total 5-year survival rate, which is still as low as 5% (1). More recently, agents targeted against molecular determinants of cancer cells or tumor vessels, or both, have been tested successfully in clinical trials to expand the therapeutic spectrum (2–4). However, to take full advantage of targeted therapies, it is essential to achieve a more profound knowledge of the molecular determinants of tumor development and progression.

The biological aggressiveness of pancreatic cancer is defined by its local invasion, tumor angiogenesis, and its potential to metastasize. To address these key events by targeted therapy, recent efforts have focused on the identification of molecular indicators of disease progression. The role of angiogenesis in pancreatic cancer progression has been studied extensively in the last years. However, data on specific molecular changes of tumor cells that eventually lead to a more metastatic and angiogenic phenotype depend strongly on the experimental systems used.

EFEMP1 (epidermal growth factor–containing fibulin-like extracellular matrix protein 1, fibulin-3) is a member of the fibulin family of extracellular glycoproteins, which are characterized by a tandem array of epidermal growth factor–like repeats and the fibulin-type COOH-terminal module. Fibulins are widely distributed and often associated with vasculature and elastic tissues (5). In cancer, diverse functions of the members of the fibulin family have been reported (6). Whereas fibulin-1 was shown to mediate chemoresistance in breast cancer and furthermore seems to play a role in tumor immunosurveillance (7, 8), loss of fibulin-2 results in breast cancer progression (9). Other reports imply a role of the fibulins in colon cancer tumorigenesis and breast cancer epithelial-mesenchymal transition (10, 11).

Recently, EFEMP1 has been associated with inherited forms of macular degeneration (12, 13). Specifically in these conditions, a single mutation in the EFEMP1 gene (Arg-345 to Trp) results in an aberrant accumulation of EFEMP1 protein in the endoplasmic reticulum of retinal pigment epithelial cells

Received 3/10/08; revised 10/6/08; accepted 11/5/08; published OnlineFirst 02/10/2009.

Grant support: Deutsche Forschungsgemeinschaft grant KFO 128/1-1 (C.J. Bruns). The costs of publication of this article were defrayed in part by the payment of page charges. This article must therefore be hereby marked *advertisement* in accordance with 18 U.S.C. Section 1734 solely to indicate this fact.

Note: H. Seeliger and P. Camaj contributed equally to this work.

Requests for reprints: Hendrik Seeliger, Munich University Medical Center, Department of Surgery, Marchioninstr. 15, D-81377 Munich, Germany. Phone: 49-89-7095-0; Fax: 49-89-7095-8893. E-mail: hendrik.seeliger@med.uni-muenchen.de

Copyright © 2009 American Association for Cancer Research. doi:10.1158/1541-7786.MCR-08-0132

(12). In mutated *EFEMP1*, an up-regulation of vascular endothelial growth factor (VEGF) expression is created by a protein misfolding that activates the unfolded protein response signaling pathway (14, 15). Loss of *EFEMP1*, however, does not result in macular degeneration but in the appearance of hernias as a consequence of a reduction of elastic fibers of fascial connective tissue (16). Interestingly, when originally isolated in senescent fibroblasts, *EFEMP1* was observed to be decreased by mitogenic culture conditions; however, when microinjected into fibroblasts, DNA synthesis was stimulated consistently in an autocrine and paracrine manner (17).

As fibulin effects on cell proliferation, motility, invasion, and angiogenesis may be context sensitive (18, 19), we were interested to see whether *EFEMP1* had an influence on pancreatic adenocarcinoma progression. In this study, we hypothesize that *EFEMP1* expression is up-regulated in pancreatic adenocarcinoma as a part of a network of genes that promote tumor growth and angiogenesis. For this purpose, we assessed differentially expressed genes in FG, a human pancreatic adenocarcinoma cell line that *in vivo* forms tumors that typically display a modest growth and do not metastasize, as well as L3.6pl, a variant of FG that has been characterized by aggressive tumor growth, formation of liver metastases, and extensive tumor angiogenesis (20). Further, we show that *EFEMP1* overexpression in FG cells results in enhanced tumor growth by inhibition of tumor cell apoptosis and stimulation of angiogenesis.

Results

EFEMP1 Expression Is Up-Regulated in L3.6pl Cells

The transcriptomes of nonmetastatic FG cells and metastatic L3.6pl cells under cell culture conditions were assessed by mRNA microarray hybridization. All arrays (three biological replicates per cell line) showed comparable overall expression levels and were adequate for statistical analysis (data not shown). Of a total of 54,675 probe sets, 21,172 (38%) showed a present call in at least one treatment group and were used to determine differentially expressed genes. We identified 36 genes that were up-regulated in L3.6pl cells, compared with FG, with a fold change of >1.5 (Table 1). Among these, *EFEMP1* showed a 6.45-fold up-regulation. This result was confirmed by quantitative real-time reverse transcription-PCR (RT-PCR), showing an 8.53-fold up-regulation of *EFEMP1* in L3.6pl cells compared with FG cells. Further, the IFN (α , β , and ω) receptor 1 (*IFNAR1*), *STAT1*, *I κ B- ζ* , and *IFIT3* were shown to be up-regulated in L3.6pl cells, suggesting a link to inflammation signaling pathways.

Differential Expression of *EFEMP1* in FG and L3.6pl Cells *In vivo* and *In vitro*

To assess the differential expression of *EFEMP1* in FG and L3.6pl cells in an *in vivo* tumor system, tumors arising from both cell lines were grown orthotopically in nude mice. On necropsy of the animals 28 days after tumor cell inoculation, tumors were harvested and stained for *EFEMP1*. In accordance with the microarray data, *EFEMP1* expression was more pronounced in L3.6pl tumors than in FG tumors (Fig. 1A-D). On a cellular level, *EFEMP1* was distributed homogeneously within the cytoplasm (Fig. 1D). Little is known about the

regulation of *EFEMP1* expression in cancer. Because the microarray analyses had revealed an up-regulation of several mediators of inflammation pathways in L3.6pl cells and inflammatory cells have been reported to be involved in the development and progression of pancreatic cancer (21, 22), we became interested in whether there was a link between IFN- α as a potent inflammatory stimulus and *EFEMP1* expression in tumor cells. Interestingly, IFN- α provoked a >4-fold increase of *EFEMP1* expression, as shown by quantitative RT-PCR (Fig. 2). Blockage of nuclear factor- κ B (NF- κ B) with BAY11-7082 potently inhibited both native and IFN- α -stimulated *EFEMP1* expression, indicating that IFN- α has a crucial function in the transcriptional regulation of *EFEMP1*.

EFEMP1 Overexpression Results in Enhanced Orthotopic Tumor Growth

To dissect the effects of *EFEMP1* expression on orthotopic tumor growth more specifically, we transfected the *EFEMP1* gene into FG cells (Fig. 3A). When tumor growth was analyzed *in vivo*, FG-*EFEMP1* cells consistently showed a faster orthotopic tumor growth compared with FG cells; however, FG-*EFEMP1* tumors grew less aggressively than L3.6pl tumors (Fig. 3B and C). Incidence of hepatic and lymph node metastases was similar in FG-*EFEMP1* and L3.6pl tumors (Fig. 3D). On histologic examination, H&E-stained sections of L3.6pl tumors showed extensive central necroses and strands of stromal tissue throughout the tumor. In contrast, in FG tumors, central necroses were apparent, but fibrotic areas were much less pronounced. Interestingly, FG-*EFEMP1* tumors lacked fibrotic areas, and necroses were detectable, but to a lesser extent than in FG or L3.6pl tumors (Fig. 3E-G). Because L3.6pl is highly angiogenic in comparison with FG (20), we were interested in whether *EFEMP1* overexpression had a stimulating effect on tumor angiogenesis.

EFEMP1 Expression Indirectly Stimulates Tumor Angiogenesis by VEGF Production

To elucidate potential proangiogenic effects of *EFEMP1* expression, we first analyzed the VEGF production of tumor cells. In accordance with an increase of *in vivo* angiogenesis in FG-*EFEMP1* tumors, *EFEMP1*-transfected FG cells showed a marked increase in VEGF secretion compared with vector controls (Fig. 4A). In contrast, *EFEMP1*-transfected L3.6pl cells did not show an increase of VEGF production compared with vector controls, indicating that in L3.6pl cells VEGF production is already maximally stimulated by mechanisms independent of *EFEMP1*; thus, no additional effect can be achieved. Interestingly, when assessing endothelial cell proliferation and migration, no direct stimulating effect of *EFEMP1* protein was detectable (Fig. 4B and C). In the tumor specimens, the number of CD31-positive vessels was significantly higher in tumors originating from FG-*EFEMP1* cells than from FG cells, indicating a biological proangiogenic effect of *EFEMP1* expression (Fig. 4D-G).

EFEMP1 Expression Rescues Tumor Cells from Apoptosis and Promotes Cell Cycle Progression

The relative reduction of intratumoral necroses in the xenografts formed by *EFEMP1*-transfected cells then led to

Table 1. Differentially Expressed Genes in FG versus L3.6pl Cells *In vitro*

Item_name	Fold change	Title	Gene symbol
244758_at	1.561	Zinc finger protein 452	ZNF452
223220_s_at	1.665	Poly(ADP-ribose) polymerase family, member 9	PARP9
205483_s_at	1.675	IFN, α -inducible protein (clone IFI-15K)	GIP2
216252_x_at	1.702	Fas (tumor necrosis factor receptor superfamily, member 6)	FAS
211137_s_at	1.755	ATPase, Ca ²⁺ transporting, type 2C, member 1	ATP2C1
214291_at	1.792	Ribosomal protein L17/similar to dJ612B15.1 [novel protein similar to 60S ribosomal protein L17 (RPL17)]	RPL17/dJ612B15.1
218280_x_at	1.816	Histone 2, H2aa	HIST2H2AA
1555852_at	1.825		
97935_MB_at	1.831	Signal transducer and activator of transcription 1, 91 kDa	STAT1
212239_at	1.837	Phosphoinositide-3-kinase, regulatory subunit 1 (p85 α)	PIK3R1
219234_x_at	1.912	Secernin 3	SCRN3
225669_at	2.005	IFN (α , β , and ω) receptor 1	IFNAR1
227249_at	2.089	Myosin, heavy polypeptide 11, smooth muscle	MYH11
241916_at	2.104	Phospholipid scramblase 1	PLSCR1
218736_s_at	2.121	Palmdelphin	PALMD
238035_at	2.211	Sp3 transcription factor	SP3
212764_at	2.274		
209732_at	2.308	C-type lectin domain family 2, member B	CLEC2B
221911_at	2.431	ets variant gene 1/hypothetical protein LOC221810	ETV1/LOC221810
202237_at	2.506	Nicotinamide N-methyltransferase	NNMT
226603_at	2.596	Chromosome 7 open reading frame 6	C7orf6
204160_s_at	2.662	Ectonucleotide pyrophosphatase/phosphodiesterase 4 (putative function)	ENPP4
239294_at	2.684	Transcribed locus	
231929_at	2.707	MRNA; cDNA DKFZp586O0724 (from clone DKFZp586O0724)	
204326_x_at	2.831	Metallothionein 1X	MT1X
229450_at	3.004	IFN-induced protein with tetratricopeptide repeats 3	IFIT3
201667_at	3.270	Gap junction protein, α 1, 43 kDa (connexin 43)	GJA1
229764_at	3.477	FLJ41238 protein	FLJ41238
227997_at	3.530	Interleukin-17 receptor D	IL17RD
206632_s_at	4.106	Apolipoprotein B mRNA editing enzyme, catalytic polypeptide-like 3B	APOBEC3B
223218_s_at	4.722	Nuclear factor of κ light polypeptide gene enhancer in B cells inhibitor, ζ	NFKBIZ
219511_s_at	5.341	Synuclein, α interacting protein (synphilin)	SNCAIP
204595_s_at	5.429	Stanniocalcin 1	STC1
201842_s_at	6.449	Epidermal growth factor-containing fibulin-like extracellular matrix protein 1	EFEMP1
208892_s_at	6.504	Dual specificity phosphatase 6	DUSP6
201860_s_at	86.594	Plasminogen activator, tissue	PLAT

NOTE: A fold change of >1.5 was considered significant.

the question whether *EFEMP1* expression was associated with alterations of cell death mechanisms. Under serum starvation conditions, 83.4% of FG cells underwent apoptosis. Unsurprisingly, the biologically more aggressive L3.6pl cells showed a

marked reduction of the proportion of apoptotic cells (52.3%). In FG-EFEMP1 cells, there was an even more pronounced reduction of apoptotic cells (48.0%; Fig. 5A and B). Concordant with these data, fluorescence-activated cell sorting (FACS) cell cycle analyses showed a shift from G₀-G₁ phase toward S phase and mitosis in FG-EFEMP1 cells compared with FG and L3.6pl cells, respectively (Fig. 5C). *In vivo*, fluorescent terminal deoxynucleotidyl transferase-mediated dUTP nick end labeling (TUNEL) staining of xenografts grown from FG, FG-EFEMP1, and L3.6pl cells showed a reduction of apoptotic cells in FG-EFEMP1 and L3.6pl tumors (Fig. 5D). Taken together, the findings provide evidence of either the inactivation of apoptotic signals or the stimulation of mitogenic pathways by EFEMP1.

EFEMP1 Expression Rescues Tumor Cells from Apoptosis Induced by 5-Fluorouracil, Gemcitabine, and Irinotecan

As gemcitabine, 5-fluorouracil, and irinotecan are in clinical use as cytotoxic agents in pancreatic cancer, we tested the influence of *EFEMP1* expression on apoptosis in tumor cells treated with these agents *in vitro*. Specifically, apoptotic cells were quantified by FACS after treatment with the cytotoxic substances. After treatment with 5-fluorouracil and irinotecan, respectively, a lower proportion of FG-EFEMP1 cells became apoptotic compared with FG cells (Table 2). A similar effect on

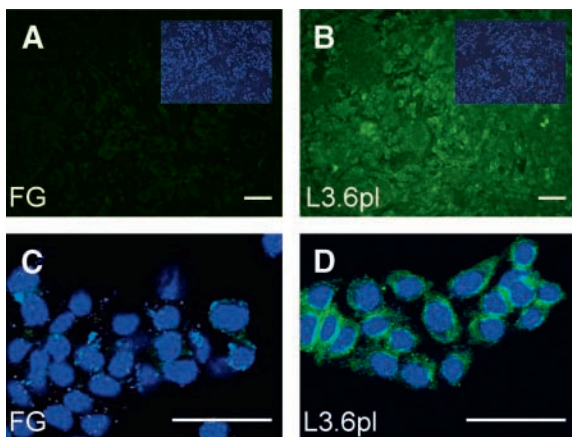


FIGURE 1. Expression of *EFEMP1* *in vivo*. Immunofluorescence of EFEMP1 expression *in vivo* in tumors originating from FG (A) and L3.6pl cells (B) 37 d after implantation. Insets, DAPI counterstain. Confocal microscopy of EFEMP1 expression in cultured FG cells (C) and L3.6pl cells (D). EFEMP1 staining (green) is increased in L3.6pl cells and follows a homogeneous perinuclear pattern. Bars, 50 μ m.

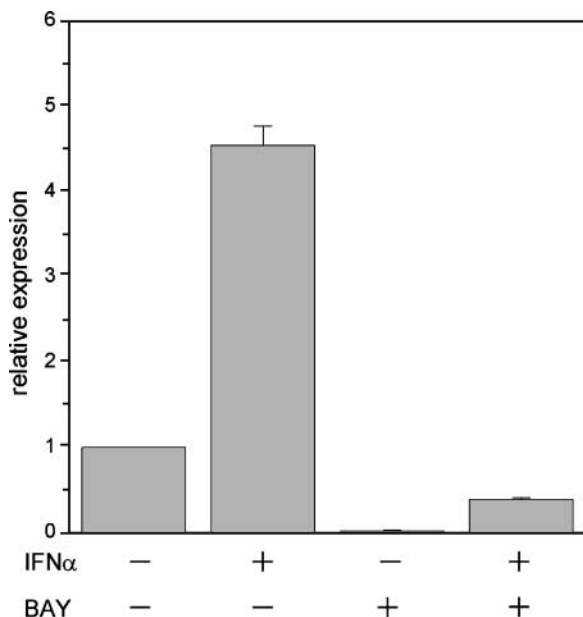


FIGURE 2. Regulation of EFEMP1 expression. Relative expression of EFEMP1 in L3.6pl cells, determined by quantitative RT-PCR. Treatment with IFN- α results in a marked up-regulation of EFEMP1 expression that is counteracted by the NF- κ B inhibitor BAY11-7082. Representative data from three independent experiments are shown.

apoptosis, although less pronounced, was observed in gemcitabine-treated cells.

EFEMP1 Expression Is Up-Regulated in Human Pancreatic Adenocarcinoma

To validate our *in vitro* and *in vivo* data in clinical human tumor specimens, EFEMP1 expression in pancreatic ductal adenocarcinoma specimens was compared with surrounding normal tissue. In 13 of 15 tumor samples (86.7%), an mRNA overexpression of EFEMP1 was seen (Fig. 6). In 12 of these, the relative up-regulation of EFEMP1 expression was >2-fold compared with corresponding nontumorous tissue. PCR followed by gel electrophoresis confirmed the quantitative results (data not shown).

Discussion

In the microarray analysis of differentially expressed genes, we showed a significant up-regulation of EFEMP1 expression in the highly metastatic L3.6pl cell line, compared with FG, for the first time. This finding was consistently substantiated *in vivo* and *in vitro* by EFEMP1 transfection of FG cells. Data generated by proteomic analyses further confirmed these results (data not shown). The influence of the tumor microenvironment on the capability of tumor cells to promote metastasis and angiogenesis is well characterized (23), resulting in different gene sets expressed when analyzing tumor cells in culture, and *in vivo* ectopic and orthotopic growth. However, a recent report on differential gene expression in FG and L3.6pl cells under *in vitro* and orthotopic *in vivo* conditions failed to detect EFEMP1 as differentially expressed in a cumulative statistical analysis, suggesting that even minute alterations of *in vitro*

culture conditions may have a significant effect on the regulation of EFEMP1 expression (24). Further, when assessing the functional properties of the EFEMP1 protein, the presence of alternative splicing variants can result in different biological functions (17). Posttranslational modification by O-glycosylation has been shown to add to the diversity of EFEMP1 depending on the set of glycosyltransferases expressed by the individual cell type (5). More strikingly, transcriptional regulation reflects the microenvironmental influences on EFEMP1 expression. We showed that IFN- α , a potent stimulus of inflammatory response, resulted in a significant up-regulation of EFEMP1 expression *in vitro* that is dependent on NF- κ B activity. In fact, there is convincing evidence that cancer and inflammation share common signaling pathways. More specifically, pancreatic adenocarcinoma and chronic pancreatitis express a substantial proportion of proteins in common (22, 25, 26), placing patients that suffer from chronic pancreatitis at risk to develop pancreatic cancer (27). Indeed, mononuclear cells as mediators of nonspecific immune responses are recruited to pancreatic cancer and result in an angiogenic phenotype of cancer cells (21). Apart from inflammation signaling, EFEMP1 expression is dependent on regulation by female sex steroids. As the EFEMP1 gene contains an estrogen-responsive element negatively regulating its transcription, treatment with 17 β -estradiol results in down-regulation of EFEMP1 protein expression (28). In this context, down-regulation of EFEMP1 in breast cancer metastasis may reflect a microenvironmental regulation in specific cancer types (29).

Stable transfection of FG cells with EFEMP1 results in a significant enhancement of orthotopic and metastatic pancreatic tumor growth, contributing to the biological validation of the differential expression analysis in an *in vivo* system. In this system, increased angiogenesis was observed and VEGF production was significantly stimulated by EFEMP1 expression, whereas EFEMP1 did not have a direct effect on endothelial cell proliferation and motility. Importantly, we were able to show the effect of EFEMP1 overexpression in an epithelial neoplasm *in vivo* for the first time. In contrast to our results, EFEMP1 overexpression in fibrosarcoma recently was shown to be associated with an inhibition of tumor growth in a s.c. model by Albig and coworkers (18). Additionally, in the same study, EFEMP1 was shown to exert antiangiogenic effects in brain microvascular cells *in vitro* and in an *in vivo* Matrigel plug assay. These at least partially conflicting findings can be explained considering the microenvironment of the different experimental settings. Our data support an indirect angiogenic effect of EFEMP1 mediated by an increase of VEGF expression and secretion. Because the more artificial Matrigel plug angiogenesis system used by Albig et al. lacks VEGF-producing tumor cells, indirect angiogenic mechanisms may not be effective compared with an orthotopic tumor model. Microenvironmental differences between the distinct tumor entities (epithelial versus mesenchymal) and the localization of tumor growth (orthotopic versus s.c.) also may be of importance in the interpretation of these discordant findings. Furthermore, the brain microvascular cells used by this group may not be representative for endothelial cells in other localizations because brain tissue typically does not express EFEMP1 (5). Tumor angiogenesis itself is the net result of the

balance between proangiogenic and antiangiogenic stimuli that greatly differ depending on tumor localization, hypoxia, and microenvironmental factors. In this context, tissue inhibitor of metalloproteinase-3, an inhibitor of matrix metalloproteinases, blocks interactions of VEGF with the VEGF-receptor 2, resulting in an inhibition of angiogenesis (30). EFEMP1 has been shown to act as a binding partner of tissue inhibitor of metalloproteinase-3 (31); yet, the functional nature of this interaction is unknown. Interestingly, the Arg345Trp mutation in the *EFEMP1* gene leads to an accumulation of misfolded EFEMP1 protein in the endoplasmic reticulum, resulting in an activation of the unfolded protein response and, consequently, an up-regulation of VEGF expression (15). It may be speculated that the overexpression of nonmutated *EFEMP1*, the existence of different splice variants, or posttranslational alterations similarly can activate the unfolded protein response, especially in combination with intratumoral hypoxia. Furthermore, temporal differences in *EFEMP1* expression in key events of angiogenesis are known (32) even if the chronological sequence yet has to be characterized more profoundly.

The balance between cell growth, survival mechanisms, and apoptosis is essential for the progression of cancer. We showed that *EFEMP1* overexpression in pancreatic adenocarcinoma is associated with a profound inhibition of apoptosis, relating EFEMP1 to cell survival mechanisms. EFEMP1 was isolated originally in senescent and quiescent fibroblasts, indicating a proapoptotic role. Interestingly, when microinjecting *EFEMP1* mRNA into young fibroblasts, a consistent stimulation of DNA

synthesis was seen (17). This observation is consistent with our findings that *EFEMP1* overexpression results in cell cycle progression rather than apoptosis.

Expanding these results by the application of cytotoxic substances commonly used in the clinical treatment of pancreatic cancer, we characterized a mechanism of EFEMP1-mediated interference with the apoptotic response toward gemcitabine, 5-fluorouracil, and irinotecan in pancreatic cancer. With all substances evaluated, we found a potent inhibition of apoptosis by *EFEMP1* expression. Induction of cell cycle arrest and apoptosis are key events in cytotoxic chemotherapy with agents interfering with DNA synthesis. Because pharmacogenomic considerations become increasingly important in clinical oncology (33), EFEMP1 may be a candidate for pretherapeutic evaluation in medical therapy of pancreatic cancer.

Finally, our data indicate that in human pancreatic adenocarcinoma, *EFEMP1* is up-regulated in tumor areas compared with corresponding normal pancreatic tissue. Taken together with the observation that *EFEMP1* overexpression stimulates VEGF production *in vivo*, our findings are concordant with reports of the up-regulation of VEGF in pancreatic cancer (34-36). In contrast to our data that support a role of EFEMP1 in tumor progression in pancreatic adenocarcinoma, *EFEMP1* expression was found down-regulated in lung cancer (37) and up-regulated in only 10% of different solid cancer entities (18). These discordant data may be caused by differences in the tumor entities examined; however, all published data on *EFEMP1* expression in human tumor samples

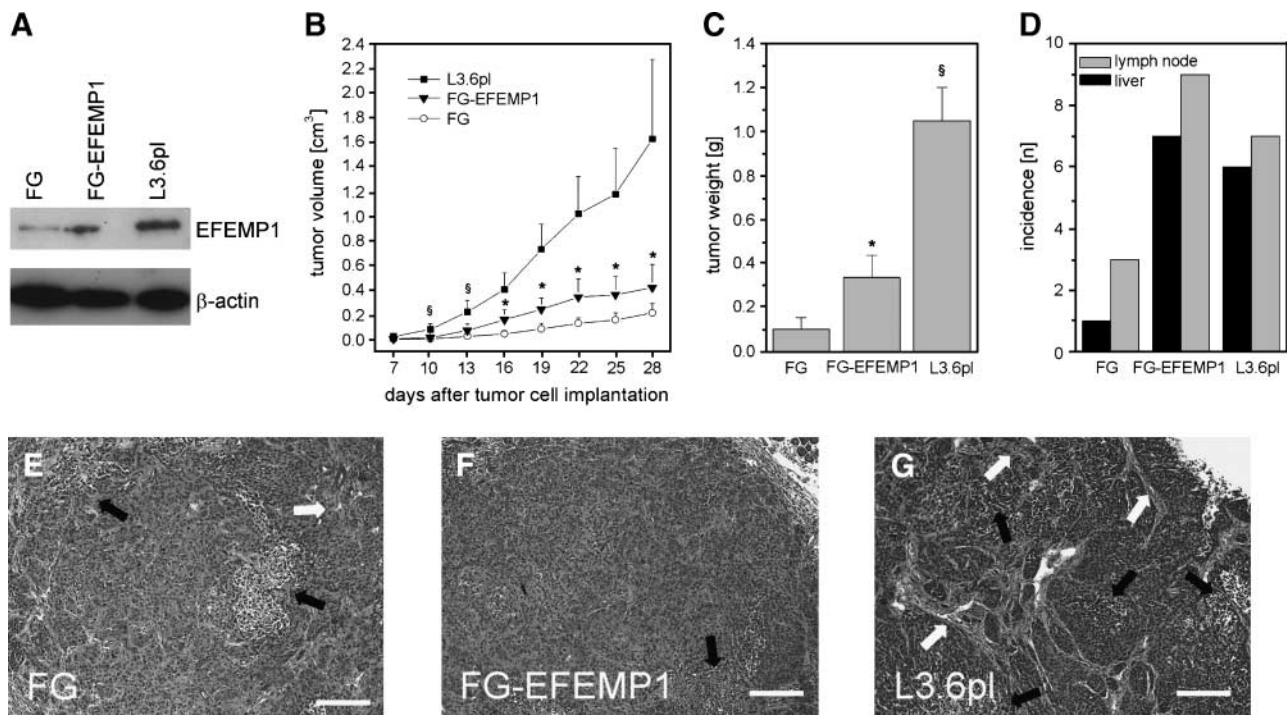


FIGURE 3. *In vivo* growth of EFEMP1-overexpressing tumors. **A.** Expression levels of EFEMP1 protein in FG, FG-EFEMP1, and L3.6pl cells. **B.** Orthotopic pancreatic tumor growth after injection of FG, FG-EFEMP1, and L3.6pl cells. FG-EFEMP1 versus FG: §, $P < 0.05$; *, $P < 0.01$. **C.** Tumor weight on necropsy 28 d after tumor cell injection. FG versus FG-EFEMP1, and FG-EFEMP1 versus L3.6pl: *, $P < 0.01$. **D.** Macroscopic incidence of hepatic and lymphogenic metastases ($n = 10$). **E** to **G.** H&E staining of FG (**E**), FG-EFEMP1 (**F**), and L3.6pl (**G**) tumors grown orthotopically. Necrosis (black arrows) and fibrotic tissue (white arrows) both are most pronounced in L3.6pl tumors. Bars, 200 μ m.

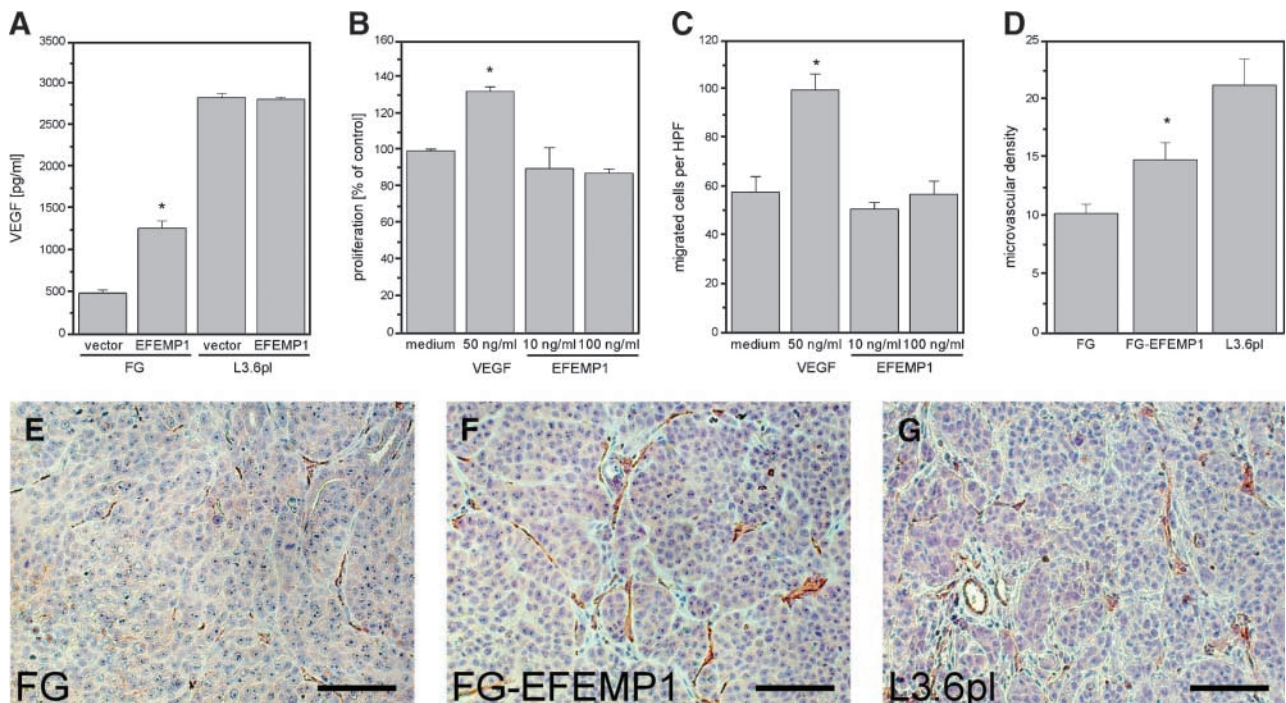


FIGURE 4. EFEMP1 induced angiogenesis. **A.** In FG-EFEMP1 transfectants, a significant increase in VEGF production was observed (*, $P < 0.01$ in FG vector controls versus FG-EFEMP1). Notably, no further stimulation of VEGF production was seen in EFEMP1-transfected L3.6pl cells compared with L3.6pl vector controls. **B.** Proliferation of HUVECs induced by VEGF-A (50 ng/mL) and EFEMP1 protein (10 and 100 ng/mL). No significant direct effect of EFEMP1 protein on the proliferation was observed. VEGF-A versus medium control; *, $P < 0.01$. **C.** Migration of HUVECs induced by VEGF-A (50 ng/mL) and EFEMP1 protein (10 and 100 ng/mL) in a modified Boyden chamber assay. Again, there was no significant direct effect of EFEMP1 protein. VEGF-A versus medium control; *, $P < 0.01$. **D.** Microvascular density is increased in tumors grown from FG-EFEMP1 cells compared with FG (*, $P < 0.05$). **E** to **G.** CD31 staining of tumor specimens grown from FG (**E**), FG-EFEMP1 (**F**), and L3.6pl cells (**G**). Bars, 100 μ m.

are limited by small sample size, thus bear a rather preliminary character. Future work should correlate *EFEMP1* expression with clinicopathologic tumor characteristics and clinical follow-up data in larger series.

In conclusion, we were able to show that EFEMP1 is up-regulated in biologically aggressive pancreatic adenocarcinoma and results in enhancement of *in vivo* orthotopic and metastatic tumor growth. EFEMP1-mediated VEGF expression contributes to the angiogenic phenotype of aggressive pancreatic cancer. Further, antiapoptotic properties of EFEMP1 mediate its protumorigenic effect and a decreased response of pancreatic cancer cells toward cytotoxic agents. The clinical validation of these data with respect to prognostic end points, as well as the role of the regulation of *EFEMP1* by inflammation pathways, represents promising targets for further investigation.

Materials and Methods

Pancreatic Cancer Cell Lines

The pancreatic cancer cell line FG is a variant of Colo357, a human pancreatic adenocarcinoma cell line originally derived from a celiac lymph node metastasis. L3.6pl is a highly metastatic and angiogenic variant of FG selected by repeated injection of metastatic cells into the spleen and pancreas of mice (20). Both cell lines were maintained in DMEM under culture conditions and with supplements as described previously (20).

RNA Sample Preparation, Microarray Hybridization, and Statistical Analysis

After harvesting FG and L3.6pl cells, total RNA was isolated with Trizol Reagent (Invitrogen) according to the manufacturer's protocol. Total RNA quantity and quality were determined by spectrometry using the NanoDrop ND-1000 spectrophotometer (NanoDrop Products) and agarose gel electrophoresis. Of each total RNA sample, 10 μ g was reversely transcribed to double-stranded cDNA using the Affymetrix One-Cycle cDNA Synthesis kit (Affymetrix). All steps were essentially done as described by the manufacturer. The cDNA was purified and transcribed into biotin-labeled cRNA using the GeneChip IVT Labeling kit (Affymetrix).

The biotinylated cRNA was purified, fragmented, and hybridized to the HG U133 Plus 2.0 GeneChip (Affymetrix) at 45°C for 16 h. The chips were washed, stained with R-phycoerythrin coupled to streptavidin (Invitrogen), and finally scanned with a GeneChip Scanner 3000 (Affymetrix). Raw data were normalized with the R program package GCRMA⁵ using default settings. For further analysis, only probe sets with a present call in at least one treatment group were used, as determined by the Data Mining Tool (Affymetrix). Differentially expressed genes were identified with significance analysis of microarrays (38). Probe sets with a fold change of >1.5 were considered as differentially expressed.

⁵ <http://www.bioconductor.org>

Cloning and Expression of the EFEMP1 Gene

The coding sequence of *EFEMP1* cDNA (OriGene Technologies) was amplified by PCR using proofreading Pfx50 DNA polymerase (Invitrogen) and inserted into the expression vector pcDNA 3.2 GW/V5 (Invitrogen). Using the primers CACAATGTTGAAAGCCCTTTTCTAACTATGCTGACTC (*EFEMP1*TOPOforw) and AAATGAAAATGGCCCCACTAT-TATTGTC (*EFEMP1*TOPOrev), the *EFEMP1* gene was cloned with and without a V5 Tag attached to the COOH terminus. Before the TOPO reaction, the PCR product was verified by restriction analysis. Absence of PCR-based mutations was confirmed by sequencing. Both pancreatic cell lines (FG and L3.6pl) were stably transfected with *EFEMP1* DNA and the empty vector, respectively, using Metafectene transfection (Biontix). Pooled stable transfectants were selected by geneticin. Expression of *EFEMP1* was verified by Western blotting.

Quantitative RT-PCR

To assess transcriptional regulation of *EFEMP1*, quantitative real-time PCR was applied to RNA extracted from cell

cultures after treatment with human recombinant IFN- α and the NF- κ B inhibitor BAY11-7082 (both Sigma-Aldrich). Total RNA was isolated using the RNeasy kit (Qiagen), RNA integrity was verified by agarose-formaldehyde electrophoresis detection of 18s and 28s rRNA, and isolated RNA was quantified by spectrophotometry using the GeneQuant Pro RNA/DNA calculator (Pharmacia). Quantitative RT-PCR for *EFEMP1* was conducted using the SuperScript III Platinum SYBR Green One-Step qRT-PCR kit (Invitrogen) with the *EFEMP1*-specific primers GAGGGGAGCAGTGCCTAGACA and TCGGCACATGGCATTGAGAC according to the manufacturer's instructions on a LightCycler system (Roche Diagnostics). PCR efficiency was assessed using the plasmid standards and quantified relative to the housekeeping gene transcript glyceraldehyde-3-phosphate dehydrogenase.

Western Blotting

For the *EFEMP1* Western blotting analysis, extracts were prepared from cultivated FG-*EFEMP1* cells. Equal amounts of protein extract were separated on polyacrylamide SDS gels,

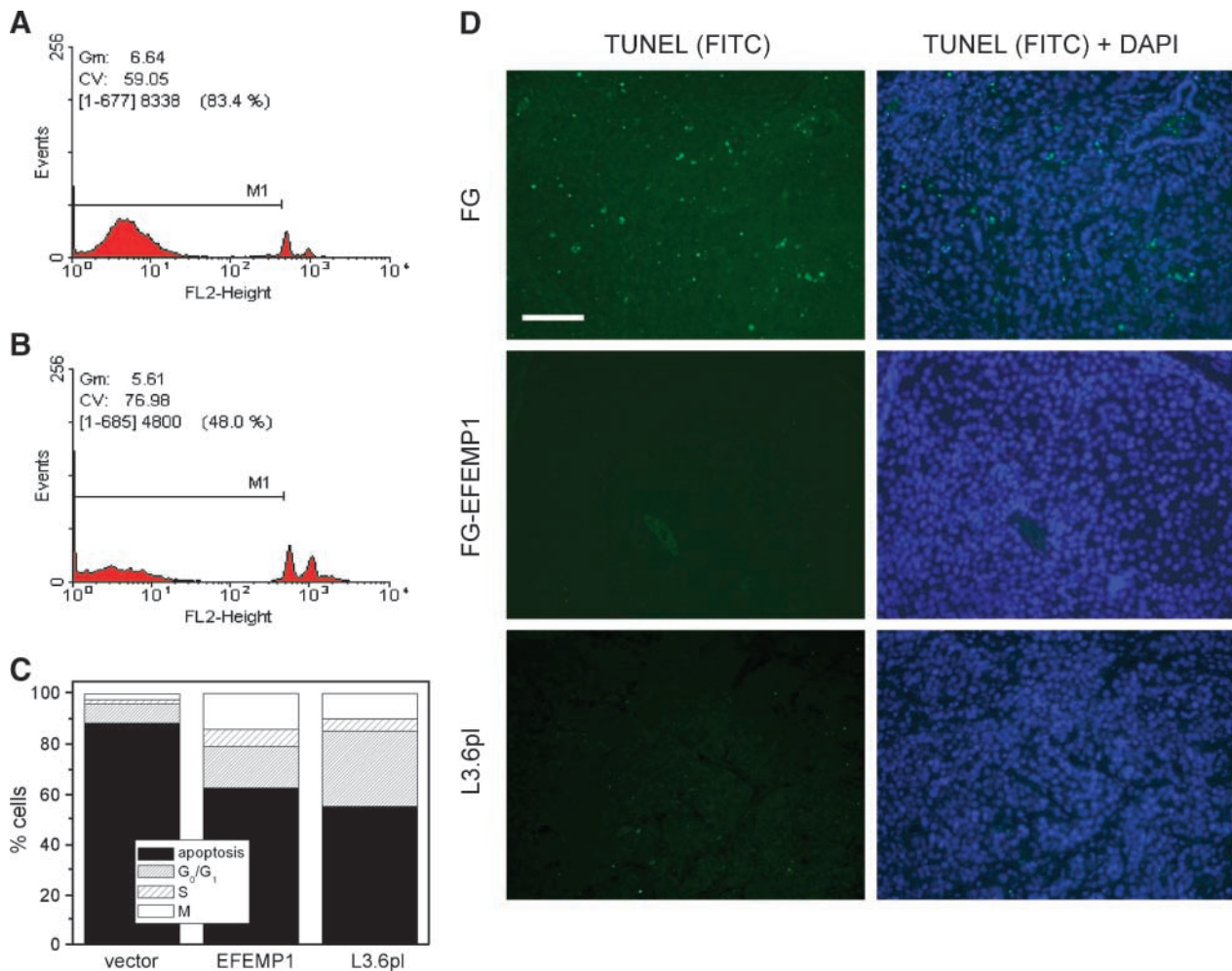


FIGURE 5. Suppression of apoptosis by *EFEMP1* expression *in vitro* and *in vivo*. Under serum starvation conditions, a FACS scan of FG vector controls (**A**) shows 83.4% apoptotic tumor cells, whereas the proportion of apoptotic FG-*EFEMP1* cells (**B**) is reduced (48.0%). Data from a typical experiment are shown. **C.** Proportions of apoptotic (solid bar), G₀-G₁-phase (dense bands), S-phase (sparse bands), and mitotic cells (white) of FG, FG-*EFEMP1*, and L3.6pl cells cultivated under serum starvation conditions. **D.** TUNEL staining of apoptotic tumor cells in xenografts of FG, FG-*EFEMP1*, and L3.6pl cells. Bar, 100 μ m.

Table 2. Apoptosis of FG, FG-EFEMP1, and L3.6p1 Cells after Treatment with Gemcitabine, 5-Fluorouracil, and Irinotecan

	FG (vector)	FG-EFEMP1	L3.6p1 (vector)
No treatment			
Apoptosis (%)	16.5	18.9	17.4
Fold change	1.00	1.00	1.00
Gemcitabine (50 ng/mL)			
Apoptosis (%)	44.3	39.9	37.3
Fold change	2.68	2.11	2.14
5-Fluorouracil (10 µg/mL)			
Apoptosis (%)	75.6	31.8	37.6
Fold change	4.58	1.68	2.16
Irinotecan (470 ng/mL)			
Apoptosis (%)	76.6	45.8	52.9
Fold change	4.64	2.42	3.04

NOTE: Proportions of apoptotic FG, FG-EFEMP1, and L3.6p1 cells as determined by FACS after treatment with gemcitabine, 5-fluorouracil, and irinotecan at their respective IC₅₀ doses (IC₅₀ determination not shown).

transferred onto a polyvinylidene difluoride membrane, and probed with a polyclonal rabbit anti-EFEMP1 antibody (AB14926, Biozol). Then, the bound primary antibody was detected with a horseradish peroxidase-conjugated secondary goat anti-rabbit antibody (Dako) using the enhanced chemiluminescence Western blotting system (Amersham).

VEGF ELISA

To assay VEGF concentrations in the supernatants of the native and *EFEMP1*-transfected cell lines, the Quantikine human VEGF ELISA kit (R&D Systems) was used according to the manufacturer's protocol. Absorbance was measured on an ELISA reader (Tecan), and VEGF content was calculated according to the calibration curve. Calibration curves with a correlation coefficient of at least 0.998 were used.

Human Umbilical Vein Endothelial Cells and In vitro Cell Proliferation and Migration Assays

Human umbilical vein endothelial cell (HUVEC) cultures were purchased from PromoCell and maintained in Falcon

“surface-modified” polystyrene flasks with growth factor-supplemented (“Supplement Pack,” PromoCell) endothelial cell basal medium (PromoCell) containing 2% fetal bovine serum, as detailed by the manufacturer.

HUVEC proliferation was measured using the colorimetric 3-(4,5-dimethylthiazol-2-yl)-2,5-diphenyltetrazolium bromide (MTT) assay (Roche Diagnostics) according to the manufacturer's protocol. Briefly, 10⁴ cells were plated into 96-well plates and cultivated for 72 h in medium containing human recombinant VEGF-A (R&D Systems) or human recombinant EFEMP1 (Biozol) at the concentrations indicated. MTT reagent was added, and absorbance was measured at 570 nm. Each experiment was done thrice.

Migration of HUVECs was assessed using a modified Boyden chamber assay. HUVECs (6 × 10⁴ per well) were seeded into the upper well of a chamber system (Becton Dickinson Falcon cell culture insert; BD Biosciences) on a fibronectin-coated (Sigma-Aldrich) polyethylene terephthalate membrane with 8-µm pores. VEGF-A or human recombinant EFEMP1 was added as a chemoattractant into the lower well at the concentrations indicated. Migration through the membrane was determined after 5 h of incubation at 37°C by fixing, staining, and counting the migrated cells. Each culture condition was done in triplicate.

FACS Analysis for Apoptosis and Cell Cycle

For apoptosis and cell cycle analyses, tumor cells were cultivated in six-well plates with or without treatment with 5-fluorouracil (Gry Pharma), gemcitabine (Lilly), and irinotecan (Pfizer Pharma), respectively. After washing and scraping into Nicoletti buffer, stained DNA content was analyzed by flow cytometry (FACSCalibur, BD Biosciences). Portions of apoptotic (subdiploid), G₀-G₁-phase (diploid), S-phase (more than diploid), and M-phase (tetraploid) cells were quantified using the WinDMI 2.8 software (Scripps Research Institute).

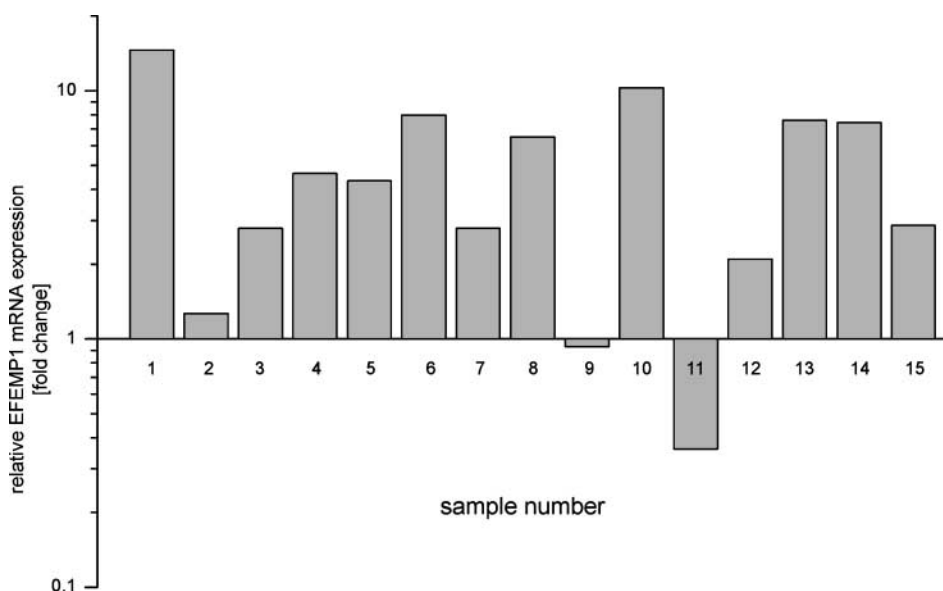


FIGURE 6. Relative expression of *EFEMP1* mRNA in human pancreatic ductal adenocarcinoma specimens. *EFEMP1* mRNA expression in the tumor and surrounding normal pancreatic tissue was compared, and individual samples are shown. *EFEMP1* mRNA expression was up-regulated in 13 of 15 tumors. Columns, mean relative mRNA expression of quantitative RT-PCR done in triplicate.

Orthotopic Tumor Injection

Male athymic *nu/nu* BALB/c mice (Charles River WIGA) were used. Animal procedures were approved by the regional authorities. For analysis of orthotopic tumor growth, FG, FG-EFEMP1, and L3.6pl cells, respectively, were injected into the pancreas of the animals, as described previously (20). Briefly, a left abdominal flank incision was made, the spleen was exteriorized, and 8×10^5 cells were injected into the sub-capsular region of the pancreas. Orthotopic tumor growth was monitored using a caliper every 2 d. On day 37 after the cell injection, animals were sacrificed and examined for orthotopic tumors, lymph node, and hepatic metastases. The tumor volume was calculated using the formula $V = \pi/6 (a \times b \times c)$, with *a*, *b*, and *c* representing length, width, and height of the mass.

Immunohistochemical Staining for EFEMP1, TUNEL, and CD31

Fluorescent immunohistochemical staining for EFEMP1 was done on paraffin-embedded tissues or tumor cells cultivated in six-well plates using a rabbit polyclonal anti-EFEMP1 antibody (Biozol) for the primary reaction. As a secondary antibody, a FITC-conjugated polyclonal anti-rabbit antibody (Dako) was used. Nuclei were counterstained with 4',6-diamidino-2-phenylindole (DAPI; Roche Diagnostics).

Fluorescent staining for apoptotic cell death (TUNEL) was done on paraffin-embedded tissue sections using the In Situ Cell Death Detection kit (Roche Diagnostics) according to the manufacturer's protocol, with a DAPI nuclear counterstaining.

Colorimetric detection of CD31 was done using a rabbit polyclonal anti-CD31 antibody (Abcam) and a biotinylated secondary goat anti-rabbit antibody (Vector Laboratories) followed by a staining reaction (NovaRED substrate kit, Vector Laboratories). Sections were counterstained with Mayer's hematoxylin.

Human Tumor Samples

The collection of human tumor tissue was approved by the local ethics committee. Operative specimens of tumor and corresponding normal tissues were obtained from 15 patients with histologically confirmed pancreatic ductal adenocarcinoma. The tissues were snap frozen and stored in liquid nitrogen. RNA extraction and quantitative RT-PCR for *EFEMP1* were done as described above. Quantitative results were normalized for glyceraldehyde-3-phosphate dehydrogenase.

Statistical Analysis

Data are given as the mean \pm SE in quantitative experiments. For statistical analysis of differences between the groups, an unpaired Student's *t* test was done.

Disclosure of Potential Conflicts of Interest

No potential conflicts of interest were disclosed.

Acknowledgments

We thank Martin Luckner, Sabine Schrepfer, and Nina Seel for their excellent technical assistance.

References

- Jemal A, Siegel R, Ward E, Murray T, Xu J, Thun MJ. Cancer statistics, 2007. *CA Cancer J Clin* 2007;57:43–66.
- Bareschino MA, Schettino C, Troiani T, Martinelli E, Morgillo F, Ciardiello F. Erlotinib in cancer treatment. *Ann Oncol* 2007;18 Suppl 6:vi35–41.
- Kindler HL, Friberg G, Singh DA, et al. Phase II trial of bevacizumab plus gemcitabine in patients with advanced pancreatic cancer. *J Clin Oncol* 2005;23:8033–40.
- Kulke MH, Blaszczak LS, Ryan DP, et al. Capecitabine plus erlotinib in gemcitabine-refractory advanced pancreatic cancer. *J Clin Oncol* 2007;25:4787–92.
- Kobayashi N, Kostka G, Garbe JH, et al. A comparative analysis of the fibulin protein family. Biochemical characterization, binding interactions, and tissue localization. *J Biol Chem* 2007;282:11805–16.
- Gallagher WM, Currid CA, Whelan LC. Fibulins and cancer: friend or foe? *Trends Mol Med* 2005;11:336–40.
- Pupa SM, Argraves WS, Forti S, et al. Immunological and pathobiological roles of fibulin-1 in breast cancer. *Oncogene* 2004;23:2153–60.
- Pupa SM, Giuffrè S, Castiglioni F, et al. Regulation of breast cancer response to chemotherapy by fibulin-1. *Cancer Res* 2007;67:4271–7.
- Yi CH, Smith DJ, West WW, Hollingsworth MA. Loss of fibulin-2 expression is associated with breast cancer progression. *Am J Pathol* 2007;170:1535–45.
- Gallagher WM, Greene LM, Ryan MP, et al. Human fibulin-4: analysis of its biosynthetic processing and mRNA expression in normal and tumour tissues. *FEBS Lett* 2001;489:59–66.
- Lee YH, Albig AR, Maryann R, Schiemann BJ, Schiemann WP. Fibulin-5 initiates epithelial-mesenchymal transition (EMT) and enhances EMT induced by TGF- β in mammary epithelial cells via a MMP-dependent mechanism. *Carcinogenesis* 2008;29:2243–51.
- Marmorstein LY, Munier FL, Arsenijevic Y, et al. Aberrant accumulation of EFEMP1 underlies drusen formation in Malattia Leventinese and age-related macular degeneration. *Proc Natl Acad Sci U S A* 2002;99:13067–72.
- Stone EM, Lotery AJ, Munier FL, et al. A single EFEMP1 mutation associated with both Malattia Leventinese and Doyme honeycomb retinal dystrophy. *Nat Genet* 1999;22:199–202.
- Harding HP, Calton M, Urano F, Novoa I, Ron D. Transcriptional and translational control in the mammalian unfolded protein response. *Annu Rev Cell Dev Biol* 2002;18:575–99.
- Roybal CN, Marmorstein LY, Vander Jagt DL, Abcouwer SF. Aberrant accumulation of fibulin-3 in the endoplasmic reticulum leads to activation of the unfolded protein response and VEGF expression. *Invest Ophthalmol Vis Sci* 2005;46:3973–9.
- McLaughlin PJ, Bakall B, Choi J, et al. Lack of fibulin-3 causes early aging and herniation, but not macular degeneration in mice. *Hum Mol Genet* 2007;16:3059–70.
- Lecka-Czernik B, Lumpkin CK, Jr., Goldstein S. An overexpressed gene transcript in senescent and quiescent human fibroblasts encoding a novel protein in the epidermal growth factor-like repeat family stimulates DNA synthesis. *Mol Cell Biol* 1995;15:120–8.
- Albig AR, Neil JR, Schiemann WP. Fibulins 3 and 5 antagonize tumor angiogenesis *in vivo*. *Cancer Res* 2006;66:2621–9.
- Schiemann WP, Blobe GC, Kalume DE, Pandey A, Lodish HF. Context-specific effects of fibulin-5 (DANCE/EVEC) on cell proliferation, motility, and invasion. Fibulin-5 is induced by transforming growth factor- β and affects protein kinase cascades. *J Biol Chem* 2002;277:27367–77.
- Bruns CJ, Harbison MT, Kuniyasu H, Eue I, Fidler IJ. *In vivo* selection and characterization of metastatic variants from human pancreatic adenocarcinoma by using orthotopic implantation in nude mice. *Neoplasia* 1999;1:50–62.
- Esposito I, Menicagli M, Funel N, et al. Inflammatory cells contribute to the generation of an angiogenic phenotype in pancreatic ductal adenocarcinoma. *J Clin Pathol* 2004;57:630–6.
- Farrow B, Sugiyama Y, Chen A, Uffort E, Nealon W, Mark Evers B. Inflammatory mechanisms contributing to pancreatic cancer development. *Ann Surg* 2004;239:763–9; discussion 9–71.
- Killion JJ, Radinsky R, Fidler IJ. Orthotopic models are necessary to predict therapy of transplantable tumors in mice. *Cancer Metastasis Rev* 1998;17:279–84.
- Nakamura T, Fidler IJ, Coombes KR. Gene expression profile of metastatic human pancreatic cancer cells depends on the organ microenvironment. *Cancer Res* 2007;67:139–48.
- Chen R, Brentmall TA, Pan S, et al. Quantitative proteomic analysis reveals

that proteins differentially expressed in chronic pancreatitis are also frequently involved in pancreatic cancer. *Mol Cell Proteomics* 2007;6:1331–42.

26. Chen R, Pan S, Cooke K, et al. Comparison of pancreas juice proteins from cancer versus pancreatitis using quantitative proteomic analysis. *Pancreas* 2007; 34:70–9.
27. Duell EJ, Casella DP, Burk RD, Kelsey KT, Holly EA. Inflammation, genetic polymorphisms in proinflammatory genes TNF-A, RANTES, and CCR5, and risk of pancreatic adenocarcinoma. *Cancer Epidemiol Biomarkers Prev* 2006;15: 726–31.
28. Blackburn J, Tarttelin EE, Gregory-Evans CY, Moosajee M, Gregory-Evans K. Transcriptional regulation and expression of the dominant drusen gene FBLN3 (EFEMP1) in mammalian retina. *Invest Ophthalmol Vis Sci* 2003;44:4613–21.
29. Minn AJ, Gupta GP, Siegel PM, et al. Genes that mediate breast cancer metastasis to lung. *Nature* 2005;436:518–24.
30. Qi JH, Ebrahem Q, Moore N, et al. A novel function for tissue inhibitor of metalloproteinases-3 (TIMP3): inhibition of angiogenesis by blockage of VEGF binding to VEGF receptor-2. *Nat Med* 2003;9:407–15.
31. Klenotic PA, Munier FL, Marmorstein LY, Anand-Apte B. Tissue inhibitor of metalloproteinases-3 (TIMP-3) is a binding partner of epithelial growth factor-containing fibulin-like extracellular matrix protein 1 (EFEMP1). Implications for macular degenerations. *J Biol Chem* 2004;279:30469–73.
32. Bell SE, Mavila A, Salazar R, et al. Differential gene expression during capillary morphogenesis in 3D collagen matrices: regulated expression of genes involved in basement membrane matrix assembly, cell cycle progression, cellular differentiation and G-protein signaling. *J Cell Sci* 2001;114:2755–73.
33. Giovannetti E, Mey V, Nannizzi S, Pasqualetti G, Del Tacca M, Danesi R. Pharmacogenetics of anticancer drug sensitivity in pancreatic cancer. *Mol Cancer Ther* 2006;5:1387–95.
34. Itakura J, Ishiwata T, Friess H, et al. Enhanced expression of vascular endothelial growth factor in human pancreatic cancer correlates with local disease progression. *Clin Cancer Res* 1997;3:1309–16.
35. Itakura J, Ishiwata T, Shen B, Kormmann M, Korc M. Concomitant over-expression of vascular endothelial growth factor and its receptors in pancreatic cancer. *Int J Cancer* 2000;85:27–34.
36. Tang RF, Wang SX, Peng L, et al. Expression of vascular endothelial growth factors A and C in human pancreatic cancer. *World J Gastroenterol* 2006;12:280–6.
37. Yue W, Dacic S, Sun Q, et al. Frequent inactivation of RAMP2, EFEMP1 and Dutt1 in lung cancer by promoter hypermethylation. *Clin Cancer Res* 2007;13: 4336–44.
38. Tusher VG, Tibshirani R, Chu G. Significance analysis of microarrays applied to the ionizing radiation response. *Proc Natl Acad Sci U S A* 2001;98: 5116–21.

Molecular Cancer Research

***EFEMP1* Expression Promotes *In vivo* Tumor Growth in Human Pancreatic Adenocarcinoma**

Hendrik Seeliger, Peter Camaj, Ivan Ischenko, et al.

Mol Cancer Res 2009;7:189-198. Published OnlineFirst February 10, 2009.

Updated version Access the most recent version of this article at:
doi:[10.1158/1541-7786.MCR-08-0132](https://doi.org/10.1158/1541-7786.MCR-08-0132)

Cited articles This article cites 38 articles, 20 of which you can access for free at:
<http://mcr.aacrjournals.org/content/7/2/189.full#ref-list-1>

Citing articles This article has been cited by 4 HighWire-hosted articles. Access the articles at:
<http://mcr.aacrjournals.org/content/7/2/189.full#related-urls>

E-mail alerts [Sign up to receive free email-alerts](#) related to this article or journal.

Reprints and Subscriptions To order reprints of this article or to subscribe to the journal, contact the AACR Publications Department at pubs@aacr.org.

Permissions To request permission to re-use all or part of this article, use this link
<http://mcr.aacrjournals.org/content/7/2/189>.
Click on "Request Permissions" which will take you to the Copyright Clearance Center's (CCC) Rightslink site.